Progress In Electromagnetics Research Letters, Vol. 80, 83–89, 2018

Wideband Mushroom Composite Right/Left Handed Transmission Line Antenna with Cavity-Backed Substrate Integrated Waveguide

Huifen Huang* **and Sun Shuai**

Abstract—A wideband composite right/left handed transmission line (CRLH-TL) antenna with cavity-backed substrate integrated waveguide (SIW) is proposed in this letter. This proposed antenna consists of a 2×2 array of mushroom unit cells, feeding line and cavity-backed SIW. By introducing SIW structure both impedance and gain of the antenna are improved. The proposed antenna has average measured gain of 7 dBi (peak measured gain of 9.5 dBi), wide -10 dB impedance matching bandwidth of 55% from 5.4 GHz to 8.4 GHz, small size of $40\,\text{mm} \times 50 \times 4\,\text{mm}$, high integration ability, and reduced back radiation.

1. INTRODUCTION

Cavity-backed antenna has the advantages of stable pattern, high gain and small backward radiation. Compared with conventional metal cavities, the substrate integrated waveguide structure can effectively realize miniaturization, improve the integration ability of antennas, and is gradually used in the cavity-backed antennas [1, 2].

As antenna size decreases, radiation efficiency and gain of the antenna will be reduced because of lower electrical size. Compared with the conventional half-wavelength resonator, the superiority of the zeroth-order resonance (ZOR) of CRLH-TL mainly lies in its compact size because ZOR frequency and unloaded Q of the ZORs are independent of their physical lengths but only determined by the shunt components [3], and CRLH-TL also has advantages of broad bandwidth, low loss and multi-band resonances [4, 5]. The periodic repetition of a metallic mushroom structure, originally proposed by Sievenpiper et al. was designed as an electromagnetic bandgap (EBG) structure to suppress unwanted surface waves within a certain frequency bandgap [6]. Sanada et al. demonstrated that this structure can also be analyzed as composite right/left-handed (CRLH) TL, capable of exhibiting a negative refractive index in the left-handed bands [7]. Multiple resonant modes can be excited to achieve multi-resonances by adjusting the number of CRLH unit cells. Lots of researches have utilized mushroom structures as ZOR radiators, which achieve both wide bandwidth and high gain [8–11].

In this letter, an antenna with high gain, wide bandwidth, low profile and high integration ability is developed by combining a mushroom antenna and an SIW structure. The proposed antenna consists of a 2×2 array of mushroom unit cells, which acts as a CRLH-TL radiator, a microstrip feeding line, and an SIW structure. The SIW cavity is formed by connecting the upper patch around the mushroom cells and the ground plane by metallic vias. As indicated by simulation, SIW structure elevates the antenna gain by over 2 dBi and improves antenna impedance as well. As a result, the proposed mushroom CRLH-TL antenna with cavity-backed SIW is obtained with wide bandwidth of 55% and peak simulated gain of 9.9 dBi. In Section 1, a brief introduction of CRLH-TL and SIW researches is made. Geometry and design of the proposed antenna are explained in Section 2, while in Section 3 detailed analysis of CRLH-TL and SIW structure that this paper adopts is implemented. In Section 4 measured results are presented. Finally in Section 5 conclusion of this paper is drawn.

Received 5 September 2018, Accepted 12 November 2018, Scheduled 5 December 2018

* Corresponding author: Huifen Huang (huanghf@scut.edu.cn).

The authors are with the School of Electronics and Information Engineering, South China University of China, Guangzhou 510641, China.

2. ANTENNA GEOMETRY AND DESIGN

Figures 1(a) and (b) are top and bottom side views of the proposed antenna, respectively, and related parameters are marked in the figure. The proposed antenna consists of a 2×2 array of mushroom unit cells, a microstrip feeding line and SIW cavity. The four mushroom unit cells, feeding line and "⊓" shape patch are on the top side, and the ground plane is on the bottom side of the substrate. The "⊓" shape patch and ground plane are connected by metallic vias which form SIW cavity. The mushroom unit cells act as a CRLHTL ZOR radiator and are fed by the feeding line through gap coupling.

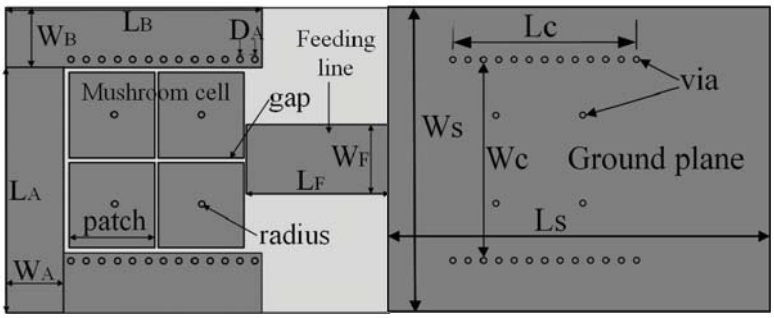

Figure 1. Geometry of the proposed antenna. (a) Top view. (b) Bottom view.

Figure 2 shows the 3D view of the mushroom structure and its equivalent circuit. A mushroom unit cell is a metal cap connected to the ground by a metal via. The mutual capacitance formed by the adjacent mushroom caps introduces series capacitance C_L, while the metal via provides shunt inductance L_L. The distributed inductor of the cap introduces series inductance L_R, while the capacitor between the ground plane and the cap introduces shunt capacitance C_R.

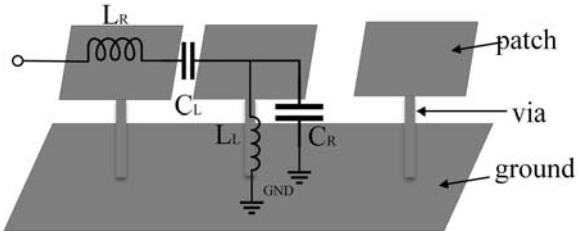

Figure 2. The mushroom schematic and its equivalent circuit model.

The proposed antenna is made on a substrate with dielectric constant of 2.2 and size of 40 mm × 50 mm × 4 mm. The design was simulated in high frequency structure simulator (HFSS) 15.0. According to antenna impedance and gain results, the optimized geometry parameters are obtained as follows: $W_S = 40\,\text{mm}$, $L_S = 50\,\text{mm}$, $L_A = 32\,\text{mm}$, $W_A = 5\,\text{mm}$, $L_B = 34\,\text{mm}$, $W_B = 8\,\text{mm}$, $D_A = 2\,\text{mm}$, $radius = 0.5\,\text{mm}$, $gap = 0.4\,\text{mm}$, $patch = 11\,\text{mm}$, $L_F = 18.82\,\text{mm}$, $W_F = 11\,\text{mm}$, $L_C = 24\,\text{mm}$, $W_C = 26.4\,\text{mm}$.

3. ANTENNA ANALYSIS

3.1. Theory of CRLH Resonator

When a CRLH-TL is not terminated to a matched load, it is transformed into a resonator where standing wave is produced. For a resonator of length l consisting of N unit cells with p period, the resonant

frequencies occur where l is multiple of half a wavelength (λ), or the electrical length is a multiple of π.

$$\beta_m l = \left(\frac{2\pi}{\lambda}\right)\left(\frac{m\lambda}{2}\right) = m\pi, \qquad m = 0, \pm 1, \ldots, \pm N - 1 \tag{1}$$

Substitute $l = Np$ into Equation (1):

$$\beta_m = \frac{m\pi}{Np} \tag{2}$$

where l is the resonator physical length, β_m the propagation constant, and m the mode number. CRLH resonant modes are achieved when $m = 0, \pm 1, \pm 2, \ldots, \pm N - 1$. Obviously, $2N - 1$ CRLH resonances are achieved from an N-cell CRLH resonator. In addition, there is another inherent TM_{10} resonance of the rectangular metallic patch which is located near the edge of the first positive-order resonance mode. Therefore, $2N$ resonances are accessible from an N-cell CRLH resonator [12].

3.2. Dispersal Characteristics Analysis

To analyze the dispersal characteristics of mushroom unit cell in Fig. 1, two-port terminal simulation for unit cell in PEC and PMC boundaries is implemented to extract the scattering parameters. With simulated scattering parameters, a dispersion diagram is presented in Fig. 3 calculated by (with period p) [13]:

$$\beta p = a\cos\left[\frac{1 - S_{11}S_{22} + S_{12}S_{21}}{2S_{21}}\right] \tag{3}$$

According to the group velocity ($\nu_g = \frac{\partial w}{\partial \beta}$) and phase velocity ($\nu_p = \frac{w}{\beta}$) definitions, LH band starts from 2 to 3.5 GHz where the phase and group velocities are out of phase, $\nu_p \nu_g < 0$. On the contrary, RH band starts from 4.5 to 7 GHz where the phase and group velocities are in-phase $\nu_p \nu_g > 0$. Based on the theory in Subsection 3.1, ZOR is in the band range 3.5–4.5 GHz, and the TM_{10} resonant mode is located near the edge of the first positive-order resonance at about 7.5 GHz as marked in Fig. 3.

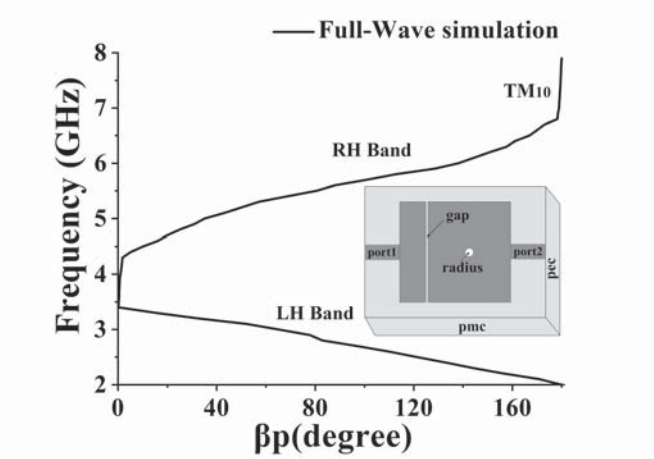

Figure 3. Dispersion diagram of single 1-D mushroom model.

3.3. Resonance Mode Analysis

Figure 4 lists the comparison of mushroom antennas with/without metallic vias and the proposed antenna. Corresponding simulated reflection coefficients are presented in Fig. 5. S_{11} of antennas a and b indicate that there is no left-handed resonance when vias are removed. For the antenna in Fig. 4(b), multiple of resonances are observed as assumed by the theory in Subsection 3.1. This mushroom antenna has quite wide bandwidth, but the reflection coefficient around 6 GHz is quite poor. On the basis of this, the SIW structure is introduced to improve impedance matching as shown in Fig. 4(c),

and TE eigenmode resonance for the SIW cavity is introduced. The resonant frequency is calculated as follows [14]:

$$f_{mn} = \frac{1}{2\sqrt{\epsilon\mu}}\sqrt{\left(\frac{m}{L_{eff}}\right)^2 + \left(\frac{n}{W_{eff}}\right)^2} \tag{4}$$

$$L_{eff} = L_c - 1.08\frac{d^2}{D_A} + 0.1\frac{d^2}{L_c} \tag{5}$$

$$W_{eff} = W_c + 0.1\frac{d^2}{W_c} \tag{6}$$

where ε and μ are the permittivity and permeability of the substrate; d is the diameter of SIW via; m and n are the standing wave numbers along x- and y-axis directions, respectively; and L_{eff} and W_{eff} represent the effective length and width of the SIW cavity, respectively. The resonant frequency of the SIW is calculated at about 5.8 GHz. As indicated in Fig. 5, reflection coefficient of the antenna is much improved after SIW is introduced especially for frequency around 6 GHz. Fig. 6 lists impedance curves of antenna b and the proposed antenna c. The capacitive reactance around 6 GHz is offset by the inductance introduced by the SIW structure, and the resistance is also improved. As a result, the impedance bandwidth is obviously broadened, which starts from 5.2 GHz to 8.3 GHz.

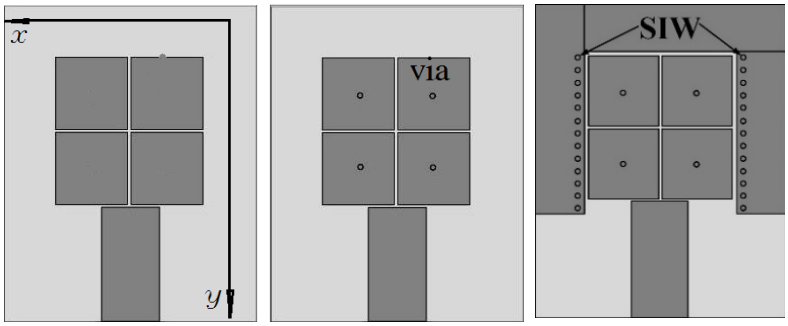

Figure 4. Constructing process of the proposed antenna. (a) Mushroom without via. (b) Mushroom without cavity-backed SIW. (c) Proposed antenna.

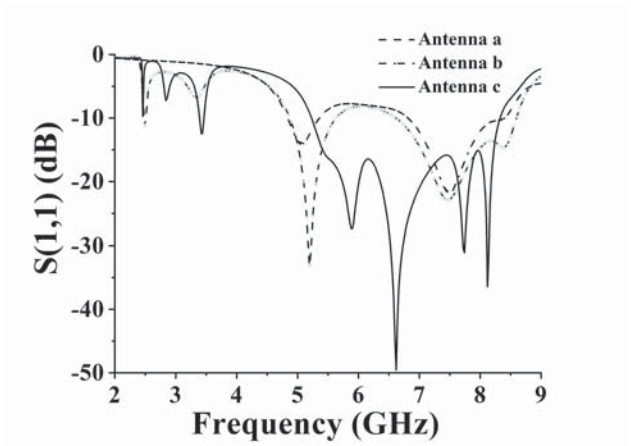

Figure 5. Simulated reflection coefficient of antennas a, b and c.

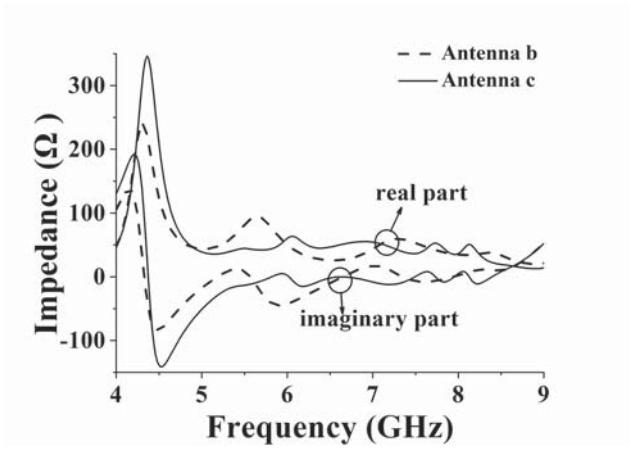

Figure 6. Simulated impedance curves of antennas b and c.

3.4. SIW Cavity-Backed Effect

SIW structure in this design also acts as a metallic cavity which blocks EM wave from radiating away from lateral sides to converge the radiation beam. Fig. 7 illustrates simulated gain results for antennas with/without SIW. As indicated by the figure, in most band antenna gain is enhanced after SIW structure is introduced, and average gain enhancement of 2 dB is obtained. Fig. 8 illustrates the far-field radiation gain patterns in E-plane of two antennas. Obviously, radiation beam is narrowed, and backward radiation is also reduced with SIW structure introduced.

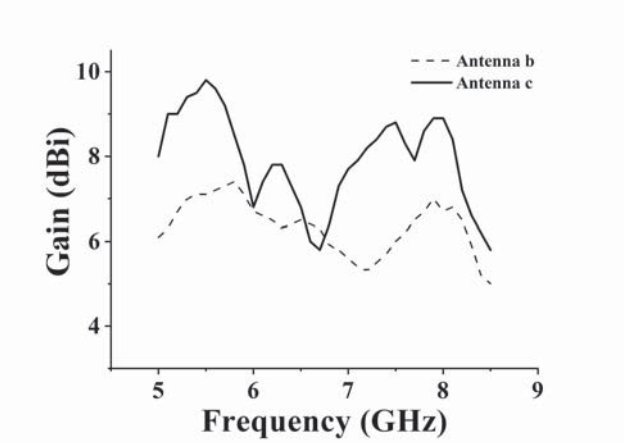

Figure 7. Simulated peak gain results of antenna b and antenna c.

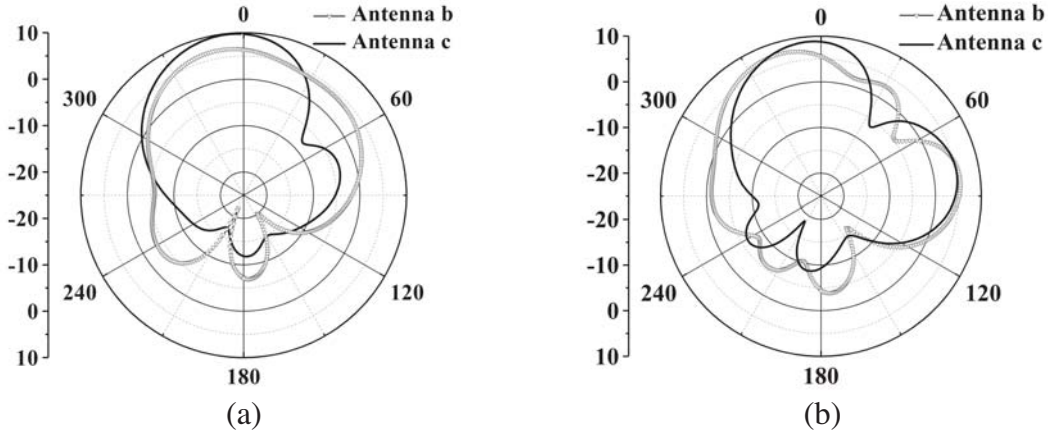

Figure 8. Gain patterns of antenna b and antenna c at 5.5 GHz (a) and 8 GHz (b) in E-plane.

4. SIMULATED AND MEASURED RESULTS

This proposed antenna is fabricated on a substrate with thickness of 4 mm and dielectric constant of 2.2 as shown in Fig. 9. Simulated and measured S_{11} in Fig. 10 are basically in agreement, and -10 dB measured impedance bandwidth from 5.4 to 8.35 GHz is obtained. Simulated and measured gains are also illustrated in the figure. Average gain of 7.5 dBi and peak gain of 9.5 dBi are achieved, a little lower than simulated results due to fabrication inaccuracy. Fig. 11 illustrates simulated and measured gain patterns at 5.5 GHz and 8 GHz, which are in good agreement. Table 1 shows a comparison of this antenna with other recently published mushroom antennas, which turns out that the proposed antenna has wider bandwidth and smaller size.

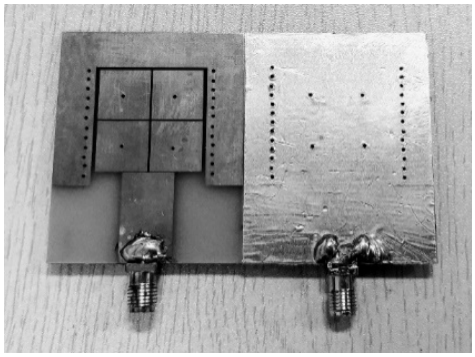

Figure 9. Fabricated prototype of the proposed antenna.

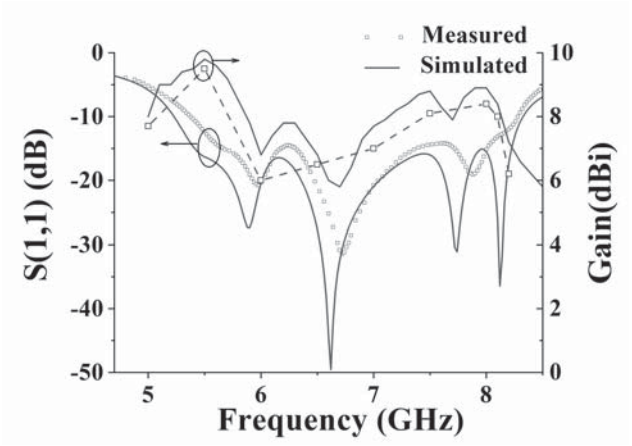

Figure 10. Simulated and measured reflection coefficients and gains of the proposed antenna.

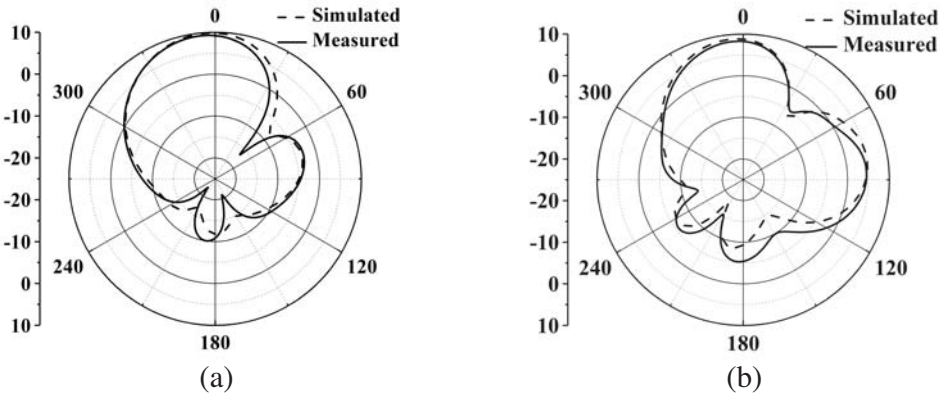

Figure 11. Simulated and measured radiation gain patterns at 5.5 GHz (a) and 8 GHz (b) of the proposed antenna in E-plane.

Table 1. Parameters of proposed antenna and previous researches.

Antenna	Bandwidth (Relative)	Gain (dBi)	Size (mm)	Units
A [8]	4.5–5.6 GHz (22%)	6–7.8	$55 * 47 * 4.8$	4×4
B [9]	4.6–6.17 GHz (28%)	7.4–10.6	$60 * 60 * 4.1$	4×4
C [10]	4.75–5.8 GHz (20%)	5–7.4	$34 * 30 * 4.2$	3×4
D [11]	4.7–6.0 GHz (25%)	8–11	$54 * 54 * 3.5$	4×4
Proposed	5.2–8.3 GHz (55%)	5.9–9.9	$50 * 40 * 4$	2×2

5. CONCLUSION

In this paper, a mushroom CRLH-TL antenna integrated with cavity-backed SIW is developed. The proposed antenna has peak measured gain of 9.5 dBi and wide -10 dB impedance bandwidth of 55% from 5.4 to 8.4 GHz in the case of minimized size after SIW structure is introduced. Compared to its predecessors, the proposed antenna has wider impedance bandwidth and smaller size.

ACKNOWLEDGMENT

This work was supported by the Key Project of Natural Science Foundation of Guangdong Province of China under Grant 2018B030311013, the Natural Science Foundation of Guangdong province under Grant 2016A030313462, the National Natural Science Foundation of China under Grant 61071056 and Characteristics of Innovation Foundation of Department of Education of Guangdong Province under Grant 2014KTSCX017.

REFERENCES

1. Deslandes, D., and K. Wu, "Accurate modeling, wave mechanisms, and design considerations of a substrate integrated waveguide," *IEEE Transactions on Microwave Theory and Techniques*, Vol. 54, No. 6, 2516–2526, 2006.
2. Honari, M. M., et al., "A dual-band low-profile aperture antenna with substrate-integrated waveguide grooves," *IEEE Transactions on Antennas and Propagation*, Vol. 64, No. 4, 1561–1566, 2016.
3. Lai, A., K. M. Leong, T. Itoh, et al., "Infinite wavelength resonant antennas with monopolar radiation pattern based on periodic structures," *IEEE Transactions on Antennas and Propagation*, Vol. 55, No. 3868-876, 2007.
4. Lee, J., "Zeroth order resonance loop antenna," *IEEE Transactions on Antennas and Propagation*, Vol. 55, No. 3, 994–997, 2007.
5. Gong, J. Q. and Q. X. Chu, "Miniaturized microstrip bandpass filter, using coupled SCRLH zeroth-order resonators," *Microwave and Optical Technology Letters*, Vol. 51, No. 12, 2985–2989, 2009.
6. Sievenpiper, D. F., et al., "High-impedance electromagnetic surfaces with a forbidden frequency band," *IEEE Transactions on Microwave Theory and Techniques*, Vol. 47, No. 11, 2059–2074, 1999.
7. Sanada, A., C. Caloz, and T. Itoh, "Planar distributed structures with negative refractive index," *IEEE Transactions on Microwave Theory and Techniques*, Vol. 52, No. 4, 1252–1263, 2004.
8. Kang, H. and S.-O. Park, "Mushroom meta-material based substrate integrated waveguide cavity backed slot antenna with broadband and reduced back radiation," *IET Microwaves, Antennas & Propagation*, Vol. 10, No. 14, 1598–1603, 2016.
9. Liu, W., Z. N. Chen, X. Qing, et al., "Metamaterial-based low-profile broadband mushroom antenna," *IEEE Transactions on Antennas and Propagation*, Vol. 62, No. 3, 1165–1172, 2014.
10. Wu, Z., L. Li, X. Chen, et al., "Dual-band antenna integrating with rectangular mushroom-like superstrate for WLAN applications," *IEEE Antennas and Wireless Propagation Letters*, Vol. 15, 1269–1272, 2015.
11. Jia, Y., Y. Liu, H. Wang, et al., "Low-RCS, high-gain, and wideband mushroom antenna," *IEEE Antennas and Wireless Propagation Letters*, Vol. 15, 277–280, 2015.
12. Amani, N. and A. Jafargholi, "Zeroth-order and TM_{10} modes in one-unit cell CRLH mushroom resonator," *IEEE Antennas and Wireless Propagation Letters*, Vol. 14, 1396–1399, 2015.
13. Liu, C., Q. Chu, and J. Huang, "A planar D-CRLH and its application to bandstop filter and leaky-wave antenna," *Progress In Electromagnetics Research Letters*, Vol. 19, 93–102, 2010.
14. Xu, F. and K. Wu, "Guided-wave and leakage characteristics of substrate integrated waveguide," *International Microwave Symposium*, Vol. 53, No. 1, 66–73, 2005.